

## 6-Deoxy- and 11-Hydroxytolypodiols: Meroterpenoids from the Cyanobacterium HT-58-2

Joshua R. Gurr, Timothy J. O'Donnell, Yuheng Luo, Wesley Y. Yoshida, Mary L. Hall, Alejandro M. S. Mayer, Rui Sun, and Philip G. Williams\*



Cite This: <https://dx.doi.org/10.1021/acs.jnatprod.9b00844>



Read Online

ACCESS |



Metrics & More

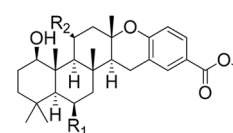
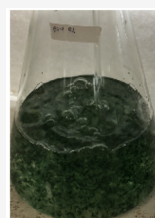


Article Recommendations



Supporting Information

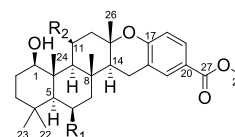
**ABSTRACT:** Chemical investigation of cyanobacterial strain HT-58-2, which most closely aligns with the genus *Brasilomena*, has led to the isolation of two compounds related to tolypodiol. The structures and absolute configuration of 6-deoxytolypodiol (**1**) and 11-hydroxytolypodiol (**2**) were elucidated by spectroscopic and spectrometric analysis. While tolypodiol previously showed anti-inflammatory activity in a mouse ear edema assay, only **2** reduced *in vitro* thromboxane B<sub>2</sub> and superoxide anion (O<sub>2</sub><sup>-</sup>) generation from *Escherichia coli* lipopolysaccharide-activated rat neonatal microglia to any appreciable degree.



6-Deoxytolypodiol (1) R<sub>1</sub> = H, R<sub>2</sub> = H  
11-Hydroxytolypodiol (2) R<sub>1</sub> = OH, R<sub>2</sub> = OH  
Tolypodiol (3) R<sub>1</sub> = OH, R<sub>2</sub> = H

Cyanobacteria are well-known producers of secondary metabolites.<sup>1</sup> The vast majority of these compounds are produced via a combination of polyketide synthase and nonribosomal peptide synthetases.<sup>1</sup> Deeper investigations into the biosynthesis of many of the peptidic compounds from cyanobacteria revealed a large number of those compounds were actually ribosomally synthesized and post-translationally modified peptides (RiPPs).<sup>1</sup> Taken together, these trends highlight the unusual nature of cultured cyanobacterial strain HT-58-2, originally classified as *Tolypothrix nodosa* based on morphology, but subsequent 16S rRNA analysis suggested it more closely resembles the genus *Brasilomena*.<sup>2</sup> While the genome contains putative clusters for several typical cyanobacterial metabolites, the two main classes of secondary metabolites expressed under a variety of culture conditions belong to neither of these structural classes. Instead, the first set of compounds, the tolyporphins, are a unique series of tetrapyrroles remarkable for their structure<sup>2</sup> and biological provenance that display potent activity as photodynamic therapy agents,<sup>3</sup> while the second class of compounds is exemplified by the meroterpenoid tolypodiols.<sup>4</sup> To date, only one naturally occurring and one synthetic derivative of this latter class of anti-inflammatory compounds have been disclosed. Reported here are results of further investigations of strain HT-58-2, which was driven primarily by our interest in exploring the tolyporphins' potential as photodynamic therapy agents given they are more potent *in vivo* than the FDA-approved drug photofrin.<sup>5,6</sup> These investigations have led to the isolation and structure elucidation of two tolypodiol analogues, 6-deoxytolypodiol (**1**) and 11-hydroxytolypodiol (**2**), from the tolyporphin-containing fraction, establishment of the absolute configurations of all members of the series (**1–3**), and biological evaluation of **1–3** in a model of pro-inflammatory mediator

inhibition with relevance to neurological disorders such as Alzheimer's disease.



6-Deoxytolypodiol (1) R<sub>1</sub> = H, R<sub>2</sub> = H  
11-Hydroxytolypodiol (2) R<sub>1</sub> = OH, R<sub>2</sub> = OH  
Tolypodiol (3) R<sub>1</sub> = OH, R<sub>2</sub> = H

From the extracts of HT-58-2 cultures, two new analogues of tolypodiol were discovered. Briefly, lyophilized biomass from HT-58-2 (43.35 g) was exhaustively extracted in 1:1 CH<sub>2</sub>Cl<sub>2</sub>/*i*-PrOH to produce an organic extract (2.33 g) after removal of solvent *in vacuo*. The residue was partitioned using a modified Kupchan partition,<sup>7</sup> and the resulting CH<sub>2</sub>Cl<sub>2</sub> extract separated using RP-flash chromatography and HPLC to yield **1** (0.5 mg), **2** (0.6 mg), and tolypodiol (**3**; 8.6 mg). The tolypodiols were minor metabolites in the extract, with tolyporphins being the most abundant metabolites.

The planar structure of **1** was determined based on conventional spectroscopic and spectrometric approaches such as LC-MS and 1D and 2D NMR based experiments. The HRESIMS of **1** produced a protonated molecule at *m/z* 441.3000 [M + H]<sup>+</sup> and established a neutral molecular

Received: September 3, 2019

formula of  $C_{28}H_{40}O_4$ . The similarity of **1** to tolypodiol, also isolated from this strain, was deduced based on resonances found in the  $^1H$  NMR spectrum consistent with five methyl signals, a methoxy group, and a 1,2,4-substituted aromatic ring. A full spectroscopic analysis of **1** revealed the lack of a hydroxy group at C-6 ( $\delta_C$  18.2) relative to tolypodiol, a modification in agreement with the molecular formula differences which established the planar structure as depicted. Further evidence of this assessment was observed in a change of multiplicity of H-5 in tolypodiol from a doublet ( $\delta_H$  0.76,  $J = 2.2$  Hz) to a doublet of doublets in **1** ( $\delta_H$  0.78,  $J = 12.1, 2.6$  Hz).

The relative configuration of the molecule was determined through analyses of 2D-ROESY correlations (Figure 1). The

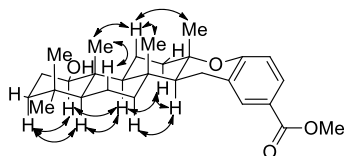


**Figure 1.** Key correlations (double-headed arrows) used to determine the relative configuration of **1**.

methine proton at C-1 was assigned an axial orientation in the ring system on the basis of an 11 Hz coupling to H-2, indicating the corresponding hydroxy group was in an equatorial orientation. Overall, the relative configuration for **1** is consistent with that reported for tolypodiol.

The planar structure of 11-hydroxytolypodiol (**2**) was deduced in a similar manner. The HRESIMS of **2** produced a protonated molecule at  $m/z$  473.2895  $[M + H]^+$  and established a molecular formula of  $C_{28}H_{40}O_6$ . The presence of an additional hydroxy group relative to tolypodiol was evident from the signal at  $\delta_H$  4.87 in the  $^1H$  NMR spectrum and was consistent with the proposed molecular formula. Analysis of the full 1D and 2D NMR data revealed this hydroxy group was in an axial orientation at C-11 based on the three small 4.8, 2.7, and 2.1 Hz couplings of proton H-11 to protons at H-9 and H<sub>2</sub>-12. Through a similar analysis of  $J_{H-H}$  coupling, the relative orientations of the carbinol protons at C-1 and C-6 were found to be the same as that observed in tolypodiol.

The absolute configurations of **1–3** were determined through ECD spectroscopy. Conformational analysis of 1R,5S,8R,9S,13S,14S-**1**, using Monte Carlo multiple minimization (MCM) with the OPLS-2005 force field in Macro-

Model, identified 10 conformers within 5 kcal/mol of the lowest energy conformer. A comparison with the experimental NMR data revealed no obvious contradictions in terms of expected coupling constants, thus validating the conformational analysis. These optimized structures and the vibrational frequencies of these conformers were subsequently calculated in Gaussian09<sup>8</sup> at the B3LYP<sup>9</sup>/DEF2SVP<sup>10</sup> level. Time-dependent density functional theory (TDDFT)<sup>11</sup> calculations were performed using Gaussian09<sup>8</sup> with six different functional and basis sets (Figure S15) to predict ECD spectra for the conformers of the 1R,5S,8R,9S,13S,14S enantiomer. The Boltzmann-weighted ECD spectrum of these conformers, calculated using SpecDis,<sup>12</sup> was compared to the experimental data for **1** at all levels. These data were in good agreement with  $\Delta_{ESI}$  values ranging from 0.875 to 0.924<sup>12</sup> and similarity factors of 0.908–0.926 and 0.0324–0.007 for the 1R,5S,8R,9S,13S,14S-configuration and its enantiomer, respectively (Figures 2A and S15). The ECD spectra of **1–3** (Figure 2B) displayed similar Cotton effects, suggesting the same absolute configuration. Slightly different  $\Delta\epsilon$  values were obtained despite our efforts to normalize the concentrations of **1** and **2** by UV (260 nm) in comparison to the more abundant **3**.

There are relatively few cyanobacterial natural products that primarily use isoprene components as building blocks.<sup>1</sup> Noscomin<sup>14</sup> and the comnostins<sup>15</sup> isolated from the media extract of *Nostoc commune* are two other examples. The closest structural relatives to the tolypodols are taondiol and its derivatives, isolated from marine brown algae, but their carbon skeletons differ with regard to substituents on the aromatic ring.<sup>16</sup>

At the time of its original isolation, tolypodiol (**3**) was shown to reduce chemically induced inflammation in an *in vivo* mouse ear edema assay<sup>4</sup> ( $ED_{50}$  30  $\mu g/ear$  for **3** vs 20  $\mu g/ear$  for the positive control). As the yields of **1** and **2** precluded testing in the original assay system, **1–3** were assessed for their effects on *in vitro* activation and generation of proinflammatory mediators by rat neonatal microglia (Figure 3) using the standard inflammation models in our laboratories.<sup>17,18</sup> Only **2** significantly inhibited the generation of proinflammatory thromboxane B<sub>2</sub> (TXB<sub>2</sub>) (apparent  $IC_{50} = 0.1 \mu M$ ). Lack of inhibition of superoxide anion ( $O_2^-$ ) generation suggests that **2** inhibits TXB<sub>2</sub> generation in rat microglia through a mechanism that may be cyclooxygenase dependent. Compound **2** is more potent in this assay system than acetylsalicylic

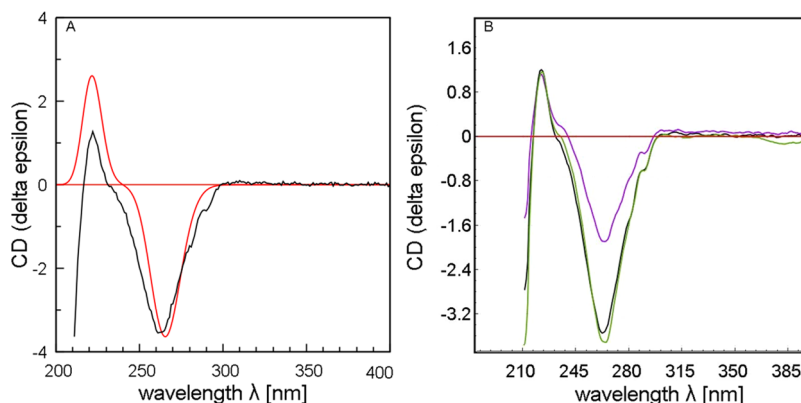


**Figure 2.** (A) Comparison of BH&HLYP<sup>10</sup>/DEF2TZVPP<sup>13</sup> calculated (red) and experimental (black) ECD curves for **1**. (B) Experimental ECD curves for 6-deoxytolypodiol (**1**; black), 11-hydroxytolypodiol (**2**; purple), and tolypodiol (**3**; green).

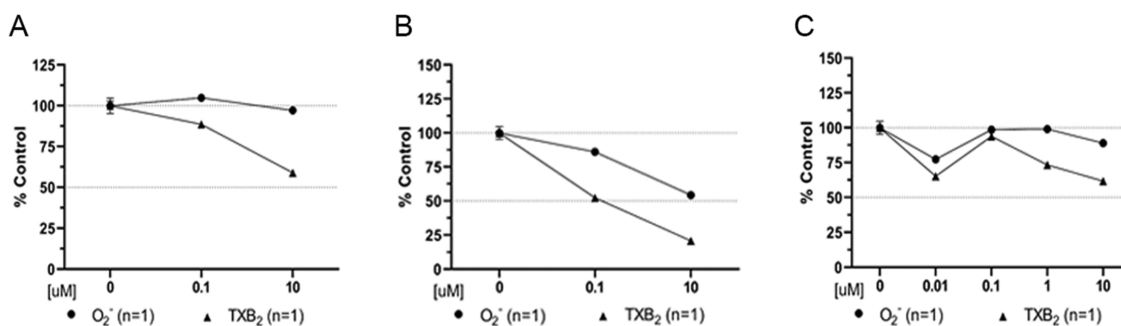


**Figure 3.** (A) Tolypodiol (3), (B) 11-hydroxytolypodiol (2), and (C) 6-deoxytolypodiol (1). PMA-stimulated  $O_2^-$  and  $TXB_2$  generation for tolypodiol, 2, and 1 were determined as described.<sup>19</sup> Data are expressed as percentage of untreated control  $O_2^-$  and  $TXB_2$  release triggered by PMA (1 mM) for 70 min. The data shown are the mean  $\pm$  SD of one independent experiment with two replicates.

acid (aspirin) ( $IC_{50}$  3.12–10  $\mu$ M), a U.S. Food and Drug Administration-approved nonsteroidal anti-inflammatory drug used to treat pain, fever, and inflammation. Further pharmacological and toxicological investigation of **2** in both *in vitro* and *in vivo* models of neuroinflammation thus appears to be warranted given modulation of  $TXB_2$  and  $O_2^-$  has been proposed as a therapeutic approach for the treatment of several neurodegenerative diseases where microglia activation has been implicated.<sup>19</sup>

In summary, two new tolypodiols analogues have been isolated and characterized from the original strain doubling the number of known members of this series. Compounds **1** and **2** differ from the previous reported analogue, tolypodiol acetate, as they differ in the oxidation state at C-6 and C-11, which suggests these modifications may occur late in the biosynthesis after the majority of the structure has been assembled. While we could not directly compare the anti-inflammatory activity of the new compounds with tolypodiol using the original assay system due to the limited quantities available, the ability of all three compounds to activate and generate proinflammatory mediators by rat neonatal microglia was determined, with only **2** showing appreciable biological activity at an apparent  $IC_{50}$  = 0.1  $\mu$ M. Compound **2** showed a level of  $TXB_2$  inhibition similar to the clinically approved NSAID flurbiprofen (apparent  $IC_{50}$  = 100 nM)<sup>20</sup> and was an order of magnitude more potent than aspirin.

## EXPERIMENTAL SECTION

**General Experimental Procedures.** Optical rotations were measured on a Jasco-DIP-700 polarimeter at the sodium line (589 nm). UV spectra were obtained on a Hewlett-Packard 8453 spectrophotometer, and IR spectra were measured as a thin film on a  $CaF_2$  disc using a PerkinElmer 1600 series FTIR. All 1D and 2D NMR spectra were acquired on a Varian Unity Inova 500 MHz spectrometer operating at 500 ( $^1H$ ) or 125 ( $^{13}C$ ) MHz using the residual solvent signals ( $\delta_H$  7.26 and  $\delta_C$  77.0) as an internal reference.  $^{13}C$  NMR spectra were acquired on a Varian Unity 600 MHz spectrometer. NMR samples were analyzed in 3 mm Shigemi NMR tubes. High-resolution mass spectrometry (HRMS) data were obtained on an Agilent 6545 LC-MS Q-ToF with ESI ionization in the positive mode. Gradient HPLC separations used a Shimadzu system consisting of LC-20AT solvent delivery modules, an SPD-M20A VP diode photodiode array detector, and an SCL-20A VP system controller.

**Cultivation of Cyanobacteria.** Cultures were revived from cryostorage and grown in BG-11 media.<sup>21</sup> Phylogenetic characterization and genomic sequencing of this strain have been previously reported.<sup>2</sup> For large-scale harvests, cultures were grown in 20 L Pyrex carboys and aerated at a flow rate of 5 L/min while under continuous

illumination of fluorescent light banks.<sup>22</sup> Cell material was harvested after 45 days of growth via decantation and filtration to be freeze-dried prior to extraction.

**Extraction and Isolation of Meroterpenes.** The lyophilized biomass from HT-58-2 (43.35 g) was exhaustively extracted in 1:1  $CH_2Cl_2/i$ -PrOH to produce an extract (2.33 g) after removal of solvent *in vacuo*. The residue was partitioned using a modified Kupchan extraction into four fractions (hexanes, 607.8 mg;  $CH_2Cl_2$ , 534.9 mg; BuOH, 28.5 mg; MeOH(aq), 100 mg). The  $CH_2Cl_2$  extract (534.9 mg) was further fractionated over C8 silica gel using a step gradient of increasing amounts of MeOH in  $H_2O$  (25%, 86.1 mg; 50%, 38.2 mg; 75%, 52.6 mg; 100% MeOH, 275.6 mg). Tolypodiol (**3**) (8.6 mg, 0.09% yield, >99% purity by UV at 265 nm,  $t_R$  18.0 min) and 11-hydroxytolypodiol (**2**) (0.6 mg, 0.007% yield, 97% purity by UV at 265 nm,  $t_R$  14.0 min) were isolated from the 75% MeOH fraction, which contained tolporphins,<sup>6,23</sup> using a linear gradient (2.7 mL/min) of  $CH_3CN$  in  $H_2O$  modified with 0.1% formic acid from 70% to 100%  $CH_3CN$  over 30 min and then 100%  $CH_3CN$  over 15 min on a Luna  $C_{18}$  (10  $\mu$ , 250  $\times$  10 mm) semipreparative column. Another portion of the 75% MeOH extract of the  $CH_2Cl_2$  partition was purified by preparative RP-HPLC (Phenomenex Luna  $C_{18}$ , 150  $\times$  21.2 mm, 5  $\mu$ m 100  $\text{\AA}$ ; with a linear gradient of  $CH_3CN$  in  $H_2O$  with 0.1% formic acid from 75% to 100%  $CH_3CN$  over 25 min and held at 100%  $CH_3CN$  for an additional 10 min; flow rate 15 mL/min) with fractions automatically collected every minute. Fractions 25 and 26 were combined from this purification and subjected to a linear gradient (3.5 mL/min) of EtOAc in hexanes from 20% to 95% over 30 min and then 100% EtOAc over 15 min on a Luna 10  $\mu$  silica (2) (100  $\text{\AA}$ , 250  $\times$  10 mm) semipreparative column, which led to the isolation of 6-deoxytolypodiol (**1**) ( $t_R$  8.1 min, 0.5 mg, 0.001% yield, >90% purity by  $^1H$  NMR).

**6-Deoxytolypodiol (1):** white, amorphous solid;  $[\alpha]_D^{22}$   $-480$  ( $c$  0.1, MeOH); UV (MeOH)  $\lambda_{max}$  (log  $\epsilon$ ) 291 (3.67), 264 (4.18) nm; ECD (1.1  $\times 10^{-4}$  M, MeOH),  $\lambda_{max}$  ( $\Delta\epsilon$ ) 262 ( $-3.5$ ), 222 (1.2) nm; IR ( $CaF_2$  disc)  $\nu_{max}$  3408, 2928, 1732, 1653, 1558, 1263  $cm^{-1}$ ; NMR data Table 1; HRESIMS  $m/z$  441.3000 [ $M + H$ ]<sup>+</sup> (calcd for  $C_{28}H_{41}O_4^+$ , 441.2999).

**11-Hydroxytolypodiol (2):** white, amorphous solid;  $[\alpha]_D^{22}$   $-160$  ( $c$  0.1, MeOH); UV (MeOH)  $\lambda_{max}$  (log  $\epsilon$ ) 290 (3.81), 264 (4.27) nm; ECD (1.1  $\times 10^{-4}$  M, MeOH),  $\lambda_{max}$  ( $\Delta\epsilon$ ) 262 ( $-1.9$ ), 222 (1.2) nm; IR ( $CaF_2$  disc)  $\nu_{max}$  3472, 2928, 2852, 1699, 1608, 1581, 1437, 1437, 1269  $cm^{-1}$ ; NMR data Table 1; HRESIMS  $m/z$  473.2895 [ $M + H$ ]<sup>+</sup> (calcd for  $C_{28}H_{41}O_6^+$ , 473.2898).

**Tolypodiol (3):** ECD (1.1  $\times 10^{-4}$  M, MeOH),  $\lambda_{max}$  ( $\Delta\epsilon$ ) 264 ( $-3.7$ ), 223 (1.2) nm.

**Biological Assay.** Rat neonatal microglia were isolated, and the assay was performed as previously described.<sup>18</sup> Primary rat neonatal microglia (200 000 cells/well) were activated with lipopolysaccharide (LPS) (0.3 ng/mL) for 17 h at 39.5  $^{\circ}C$ . Thereafter, each compound was added 20 min before microglia were stimulated with phorbol myristate acetate (PMA) at 1 mM for an additional 70 min. PMA-stimulated  $O_2^-$  and  $TXB_2$  generation were determined as described.<sup>18</sup>

**Table 1. NMR Spectroscopic Data for 1 and 2 (<sup>1</sup>H 500 MHz, <sup>13</sup>C 125 MHz, CDCl<sub>3</sub>)**

position	1		2	
	$\delta_C$ , type	$\delta_H$ (J in Hz)	$\delta_C$ , type	$\delta_H$ (J in Hz)
1	79.9, CH	3.39, dd (9.2, 6.4)	78.7, CH	3.46, dd (11.0, 5.0)
2a	30.0, CH <sub>2</sub>	1.62, m	29.0, CH <sub>2</sub>	1.79, m
2b		1.67, m		1.81, m
3a	39.7, CH <sub>2</sub>	(eq.) 1.37, m	41.4, CH <sub>2</sub>	1.35, m
3b		(ax.) 1.29, m		1.28, m
4	33.0, C		33.7, C	
5	55.0, CH	0.78, dd (12.1, 2.6)	57.1, CH	0.85, d (2.5)
6a	18.2, CH <sub>2</sub>	(eq.) 1.58, m	69.1, CH	4.52, ddd (4.0, 2.4, 1.6)
6b		(ax.) 1.50, m		
7a	40.8, CH <sub>2</sub>	(eq.) 1.78, dt (12.6, 3.2)	50.6, CH <sub>2</sub>	(eq.) 2.07, dd (14.2, 2.1)
7b		(ax.) 1.04, ddd (12.7, 12.7, 4.4)		(ax.) 1.31, dd (14.5, 4.1)
8	38.0, C		37.4, C	
9	61.2, CH	1.16, dd (11.0, 2.2)	61.2, CH	1.01, d (2.7)
10	43.6, C		43.8, C	
11a	21.3, CH <sub>2</sub>	(eq.) 2.68, ddd (14.2, 3.5, 3.5)	69.8, CH	4.87, ddd (4.8, 2.7, 2.1)
11b		(ax.) 1.47, m		
12a	41.1, CH <sub>2</sub>	(eq.) 2.06, ddd (12.6, 3.4, 3.4)	47.3, CH <sub>2</sub>	1.90, dd (13.8, 4.4)
12b		(ax.) 1.71, ddd (13.1, 13.1, 4.2)		2.34, dd (14.0, 2.7)
13	77.9, C		77.0, CH	
14	52.1, CH	1.63, m	52.7, CH	1.56, dd (13.2, 4.6)
15a	22.1, CH <sub>2</sub>	2.62, m	22.0, CH <sub>2</sub>	2.85, dd (16.3, 13.5)
15b				2.69, dd (16.6, 4.8)
16	122.1, C		122.2, C	
17	157.6, C		157.1, C	
18	116.9, CH	6.75, d (8.5)	116.8, CH	6.75, d (8.6)
19	128.9, CH	7.75, dd (8.5, 2.2)	129.0, CH	7.75, dd (8.5, 1.9)
20	121.3, C		121.2, C	
21	132.0, CH	7.78, d (2.1)	131.8, CH	7.80, d (1.2)
22	32.8, CH <sub>3</sub>	0.84, s	32.4, CH <sub>3</sub>	0.96, s
23	21.0, CH <sub>3</sub>	0.81, s	23.5, CH <sub>3</sub>	1.24, s
24	12.3, CH <sub>3</sub>	0.92, s	15.5, CH <sub>3</sub>	1.65, s
25	16.2, CH <sub>3</sub>	0.91, s	17.9, CH <sub>3</sub>	1.57, s
26	20.7, CH <sub>3</sub>	1.19, s	21.6, CH <sub>3</sub>	1.42, s
27	167.2, C		167.2, C	
28	51.7, CH <sub>3</sub>	3.86, s	51.8, CH <sub>3</sub>	3.87, s

using an immunoassay (Cayman Chemicals) according to the manufacturer's protocol. Samples were run in duplicate.

**Computational Analysis.** Conformers within 5 kcal/mol of the lowest energy conformer were searched using the MCMC method and the OPLS-2005<sup>24</sup> force field in MacroModel<sup>25</sup> (Schrodinger Inc.). Each conformer within 5 kcal/mol of the lowest energy conformer was optimized in Gaussian09<sup>8</sup> at the B3LYP<sup>26</sup>/DEF2SVP<sup>10</sup> level, and the geometries of all conformers with similar energies were checked for redundancy. Density functional theory (DFT) was used to perform calculations, which were carried out in Gaussian 09. TDDFT<sup>11</sup> calculations at several levels, including BH&HLYP<sup>10</sup>/DEF2TZVPP,<sup>13</sup> were conducted to calculate the electronic excitation energies and rotational strengths in MeOH. Boltzmann-weighted ECD spectra (Figure S15) were calculated using SpecDis<sup>12</sup> for comparison with the experimentally determined data

recorded in MeOH and to calculate similarity factors between experimental and computational spectra.

## ASSOCIATED CONTENT

### Supporting Information

The Supporting Information is available free of charge at <https://pubs.acs.org/doi/10.1021/acs.jnatprod.9b00844>.

Copies of the <sup>1</sup>H, <sup>13</sup>C, and 2D NMR spectroscopic data for all new compounds (PDF)

Spectroscopic data for all new compounds, including fids (ZIP)

## AUTHOR INFORMATION

### Corresponding Author

Philip G. Williams – Department of Chemistry, University of Hawaii at Manoa, Honolulu, Hawaii 96822, United States; [orcid.org/0000-0001-8987-0683](https://orcid.org/0000-0001-8987-0683); Phone: 808 956 5720; Email: [philipwi@hawaii.edu](mailto:philipwi@hawaii.edu); Fax: 808 956 5908

### Authors

Joshua R. Gurr – Department of Chemistry, University of Hawaii at Manoa, Honolulu, Hawaii 96822, United States

Timothy J. O'Donnell – Department of Chemistry, University of Hawaii at Manoa, Honolulu, Hawaii 96822, United States; [orcid.org/0000-0003-0291-8838](https://orcid.org/0000-0003-0291-8838)

Yuheng Luo – Department of Chemistry, University of Hawaii at Manoa, Honolulu, Hawaii 96822, United States; [orcid.org/0000-0002-3124-1179](https://orcid.org/0000-0002-3124-1179)

Wesley Y. Yoshida – Department of Chemistry, University of Hawaii at Manoa, Honolulu, Hawaii 96822, United States

Mary L. Hall – Department of Pharmacology, College of Graduate Studies Medicine, Midwestern University, Downers Grove, Illinois 60515, United States

Alejandro M. S. Mayer – Department of Pharmacology, College of Graduate Studies Medicine, Midwestern University, Downers Grove, Illinois 60515, United States; [orcid.org/0000-0002-8358-4528](https://orcid.org/0000-0002-8358-4528)

Rui Sun – Department of Chemistry, University of Hawaii at Manoa, Honolulu, Hawaii 96822, United States; [orcid.org/0000-0003-0638-1353](https://orcid.org/0000-0003-0638-1353)

Complete contact information is available at:

<https://pubs.acs.org/doi/10.1021/acs.jnatprod.9b00844>

### Notes

The authors declare no competing financial interest.

## ACKNOWLEDGMENTS

A.M.S.M. thanks L. Phelps, Z. Memedovski, and R. Schneider for expert technical assistance with the rat microglia brain cultures and for performing O<sub>2</sub><sup>-</sup> and TXB<sub>2</sub> ELISA assays and data analysis, and L. Phelps for preparing the figures. This work was supported by NIH grant 5R01AG039468 to P.W. Funds for the upgrades of the NMR instrumentation were provided by the CRIF program of the National Science Foundation (CH E9974921), the Elsa Pardee Foundation, and the University of Hawaii at Manoa. The purchase of the Agilent TOF LC-MS was funded by grant W911NF-04-1-0344 from the Department of Defense, and the purchase of the Agilent QTOF LC-MS was funded by MRI grant 1532310 from the National Science Foundation. We gratefully acknowledge the advanced computing resources provided by the University of Hawaii Information Technology Service Cyberinfrastructure, and E.

Haglund (UH Manoa) for the use of the ECD instrument. A.M.S.M. thanks the Office of Research and Sponsored Programs at Midwestern University for generous funding support for the collaborative research project.

## REFERENCES

- (1) Tidgewell, K.; Clark, B. R.; Gerwick, W. H. The Natural Products Chemistry Of Cyanobacteria. In *Comprehensive Natural Products II: Chemistry and Biology*; Elsevier Ltd, 2010; Vol. 2, pp 141–188.
- (2) Hughes, R.-A.; Zhang, Y.; Zhang, R.; Williams, P. G.; Lindsey, J. S.; Miller, S. *Appl. Environ. Microbiol.* **2017**, *83*, 1–19.
- (3) Morliere, P.; Maziere, J. C.; Santus, R.; Smith, C. D.; Prinsep, M. R.; Stobbe, C. C.; Fenning, M. C.; Golberg, J. L.; Chapman, J. D. *Cancer Res.* **1998**, *58*, 3571–3578.
- (4) Prinsep, M. R.; West, M. L.; Wylie, B. L. *J. Nat. Prod.* **1996**, *59*, 786–788.
- (5) Barnhart-Dailey, M.; Zhang, Y.; Zhang, R.; Anthony, S. M.; Aaron, J. S.; Miller, E. S.; Lindsey, J. S.; Timlin, J. A. *Photosynth. Res.* **2019**, *141*, 259–271.
- (6) Gurr, J. R.; Dai, J.; Philbin, C. S.; Sartain, H. T.; O'Donnell, T. J.; Yoshida, W. Y.; Rheingold, A. L.; Williams, P. G. *J. Org. Chem.* **2020**, *85*, 318–326.
- (7) Kupchan, S. M.; Tsou, G.; Sigel, C. W. *J. Org. Chem.* **1973**, *38*, 1420–1421.
- (8) Frisch, M. J.; Trucks, G. W.; Schlegel, H. B.; Scuseria, G. E.; Robb, M. A.; Cheeseman, J. R.; Scalmani, G.; Barone, V.; Mennucci, B.; Petersson, G. A.; Nakatsuji, H.; Caricato, M.; Li, X.; Hratchian, H. P.; Izmaylov, A. F.; Bloino, J.; Zheng, G.; Sonnenberg, J. L.; Hada, M.; Ehara, M.; Toyota, K.; Fukuda, R.; Hasegawa, J.; Ishida, M.; Nakajima, T.; Honda, Y.; Kitao, O.; Nakai, H.; Vreven, T.; Montgomery, J. A.; Peralta, J. E.; Ogliaro, F.; Bearpark, M.; Heyd, J. J.; Brothers, E.; Kudin, K. N.; Staroverov, V. N.; Kobayashi, R.; Normand, J.; Raghavachari, K.; Rendell, A.; Burant, J. C.; Iyengar, S. S.; Tomasi, J.; Cossi, M.; Rega, N.; Millam, J. M.; Klene, M.; Knox, J. E.; Cross, J. B.; Bakken, V.; Adamo, C.; Jaramillo, J.; Gomperts, R.; Stratmann, R. E.; Yazyev, O.; Austin, A. J.; Cammi, R.; Pomelli, C.; Ochterski, J. W.; Martin, R. L.; Morokuma, K.; Zakrzewski, V. G.; Voth, G. A.; Salvador, P.; Dannenberg, J. J.; Dapprich, S.; Daniels, A. D.; Farkas, Foresman, J. B.; Ortiz, J. V.; Cioslowski, J.; Fox, D. J. *Gaussian 09 Revision C.01*; Wallingford, CT, 2009.
- (9) Stephens, P. J.; Devlin, F. J.; Chabalowski, C. F.; Frisch, M. J. *J. Phys. Chem.* **1994**, *98*, 11623–11627.
- (10) Weigend, F.; Ahlrichs, R. *Phys. Chem. Chem. Phys.* **2005**, *7*, 3297–3305.
- (11) Runge, E.; Gross, E. K. U. *Phys. Rev. Lett.* **1984**, *52*, 997–1000.
- (12) Bruhn, T.; Schaumlöffel, A.; Hemberger, Y.; Bringmann, G. *Chirality* **2013**, *25*, 243–249.
- (13) Weigend, F. *Phys. Chem. Chem. Phys.* **2006**, *8*, 1057–1065.
- (14) Jaki, B.; Orjala, J.; Sticher, O. *J. Nat. Prod.* **1999**, *62*, 502–503.
- (15) Jaki, B.; Orjala, J.; Heilmann, J.; Linden, A.; Vogler, B.; Sticher, O. *J. Nat. Prod.* **2000**, *63*, 339–343.
- (16) Gonzales, A. G.; Darias, J.; Martin, J. D. *Tetrahedron Lett.* **1971**, *8*, 2729–2732.
- (17) Swanson-Mungerson, M.; Williams, P.; Gurr, J. R.; Incrocci, R.; Subramaniam, V.; Radowska, K.; Hall, M. L.; Mayer, A. M. S. *Toxicol. Sci.* **2019**, *171*, 421–430.
- (18) Klemm, L. C.; Czerwonka, E.; Hall, M. L.; Williams, P. G.; Mayer, A. M. S. *Toxins* **2018**, *10*, 10.
- (19) Aviles, E.; Prudhomme, J.; Le Roch, K. G.; Franzblau, S. G.; Chandrasena, K.; Mayer, A. M.; Rodriguez, A. D. *Bioorg. Med. Chem. Lett.* **2015**, *25*, 5339–5343.
- (20) Fiebich, B. L.; Lieb, K.; Hull, M.; Aicher, B.; van Ryn, J.; Pairet, M.; Engelhardt, G. *Neuropharmacology* **2000**, *39*, 2205–13.
- (21) Rippka, R.; Deruelles, J.; Waterbury, J. B.; Herdman, M.; Stanier, R. Y. *Microbiology* **1979**, *111*, 1–61.
- (22) Patterson, G. M. L.; Baldwin, C. L.; Bolis, C. M.; Caplan, F. R.; Karuso, H.; Larsen, L. K.; Levine, I. A.; Moore, R. E.; Nelson, C. S.; Tschappat, K. D.; Tuang, G. D.; Furusawa, E.; Furusawa, S.; Norton, T. R.; Raybourne, R. B. *J. Phycol.* **1991**, *27*, 530–536.
- (23) Minehan, T. G.; Cook-Blumberg, L.; Kishi, Y.; Prinsep, M. R.; Moore, R. E. *Angew. Chem., Int. Ed.* **1999**, *38*, 926–928.
- (24) Harder, E.; Damm, W.; Maple, J.; Wu, C.; Reboul, M.; Xiang, J. Y.; Wang, L.; Lupyan, D.; Dahlgren, M. K.; Knight, J. L.; Kaus, J. W.; Cerutti, D. S.; Krilov, G.; Jorgensen, W. L.; Abel, R.; Friesner, R. A. *J. Chem. Theory Comput.* **2016**, *12*, 281–296.
- (25) *MacroModel S.*; Macromodel LLC: New York, NY, 2019.
- (26) Becke, A. D. *J. Chem. Phys.* **1993**, *98*, 5648–5652.